Neurocomputing 177 (2016) 373–384

Contents lists available at ScienceDirect

Neurocomputing

journal homepage: www.elsevier.com/locate/neucom

Biologically inspired image enhancement based on Retinex

Yifan Wang [a], Hongyu Wang [a,*], Chuanli Yin [b], Ming Dai [b]

[a] School of Information and Communication Engineering, Dalian University of Technology, China
[b] Changchun Institute of Optics, Fine Mechanics and Physics, Chinese Academy of Sciences, China

ARTICLE INFO

Article history:
Received 2 September 2014
Received in revised form
4 February 2015
Accepted 17 October 2015
Communicated by Zhu Qingsong
Available online 29 November 2015

Keywords:
Image enhancement
Guided filter
MCNC
QDPSO
Retinex

ABSTRACT

This paper presents a biologically inspired adaptive image enhancement method, consisting of four stages: illumination estimation, reflection extraction, color restoration and postprocessing. The illumination of the input image is estimated using guided filter. We propose to utilize the smoothed *Y* channel in the YCbCr color space as the guidance image, since it can better capture the illuminance of the real scene. The reflection of the input image is extracted using the Retinex algorithm and refined through color restoration. In order to further improve the quality of the extracted reflection, we explore a learning strategy to select the optimal parameters of the nonlinear stretching by optimizing a novel image quality measurement, named as the Modified Contrast–Naturalness–Colorfulness (MCNC) function. Compared with the original CNC function, the proposed MCNC function employs a more effective objective criterion and can better agree with human visual perception. Both qualitative and quantitative experiments demonstrate that the proposed method is adaptive and robust to outdoor images and achieves favorable performance against state-of-the-art methods especially for images captured under extremely hazed or low-light conditions.

1. Introduction

In numerous applications of computer vision technology, such as visual tracking, anomaly detection and recognition, clear images are the critical prerequisite for good understanding of the real scenes. In practice, however, the quality of the images captured outdoors can be severely degraded due to various weather conditions, such as low illumination, fog and haze, which result in dimness or distortion. Therefore, enhancing and restoring degenerated images is particularly important.

Existing methods for image enhancement can be mainly classified into two categories [1]: (1) image restoration based on physical models, and (2) image enhancement based on image processing techniques.

For the first category, the optimal estimate of a haze-free image is obtained by establishing and inverting the process of image degradation. Various attempts have been explored, and tremendous progress has been made in haze removal for single image [2–4]. The dark channel prior (DCP) theory proposed by He et al. [4] directly estimates the thickness of haze using the statistics prior of haze-free outdoor images. Recent algorithms [5–7] improve the DCP method in some particular aspects. Though significant performance gain has been achieved by these methods, results restored from images captured under the overcast environment are still unsatisfactory. Take the DCP method for instance, its dehazing results are clear and natural for images with a certain brightness (Fig. 1(a) and (b)). However, it performs poorly when the lightness of the image is in the low level (Fig. 1 (c) and (d)).

The second category of image enhancement techniques directly improves contrast and highlights details by global or local pixel-processing, regardless of the cause of image degradation. Some traditional methods, such as gamma correction, contrast stretching and histogram equalization (HE), are simple but easily fail to provide exact enhanced images and sometimes may even destroy the image contents [8]. In contrast, more advanced methods, like contrast-limited adaptive histogram equalization (CLAHE) [9], wavelet transformations [10] and homomorphic filtering [8], have shown strong robustness to images of various quality.

The Retinex theory is firstly introduced to image enhancement by Land et al. [11] based on the observation that sensations of color have a strong correlation with reflectance, even though the amount of visible light reaching the eye depends on the product of reflectance and illumination. Subsequently, a line of methods [12–16] has been proposed. Among them, the multi-scale Retinex with color restoration (MSRCR) method [14] proposes to estimate the illumination of the input image using three Gaussian surround filters with different scales and conduct enhancement by applying color restoration followed by linear stretching to the logarithm of reflectance. Though the MSRCR method has demonstrated a strong ability in providing dynamic range compression and preserving

* Corresponding author.

http://dx.doi.org/10.1016/j.neucom.2015.10.124
0925-2312/

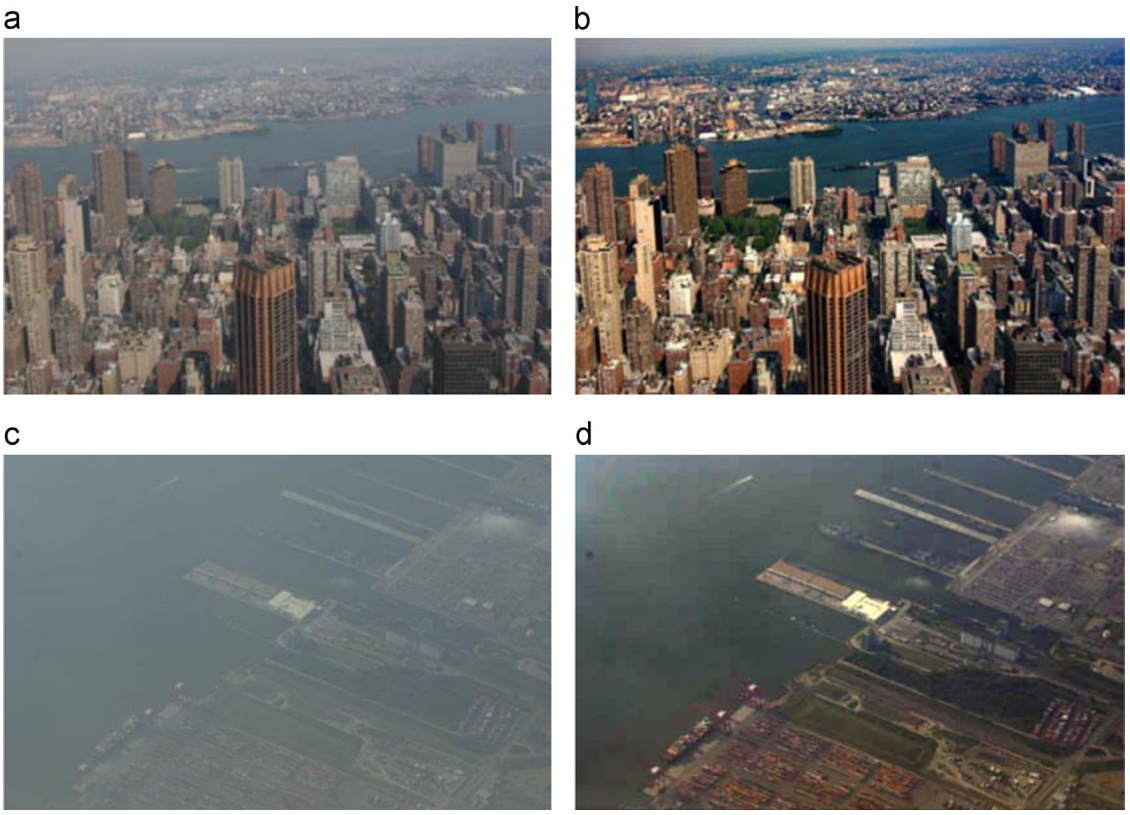

Fig. 1. DCP's success and failure. Success: for the image (a) with a certain brightness, the recovered image (b) looks nature and clear. Failure: for the low-light image (c), the result (d) is still dim with low contrast.

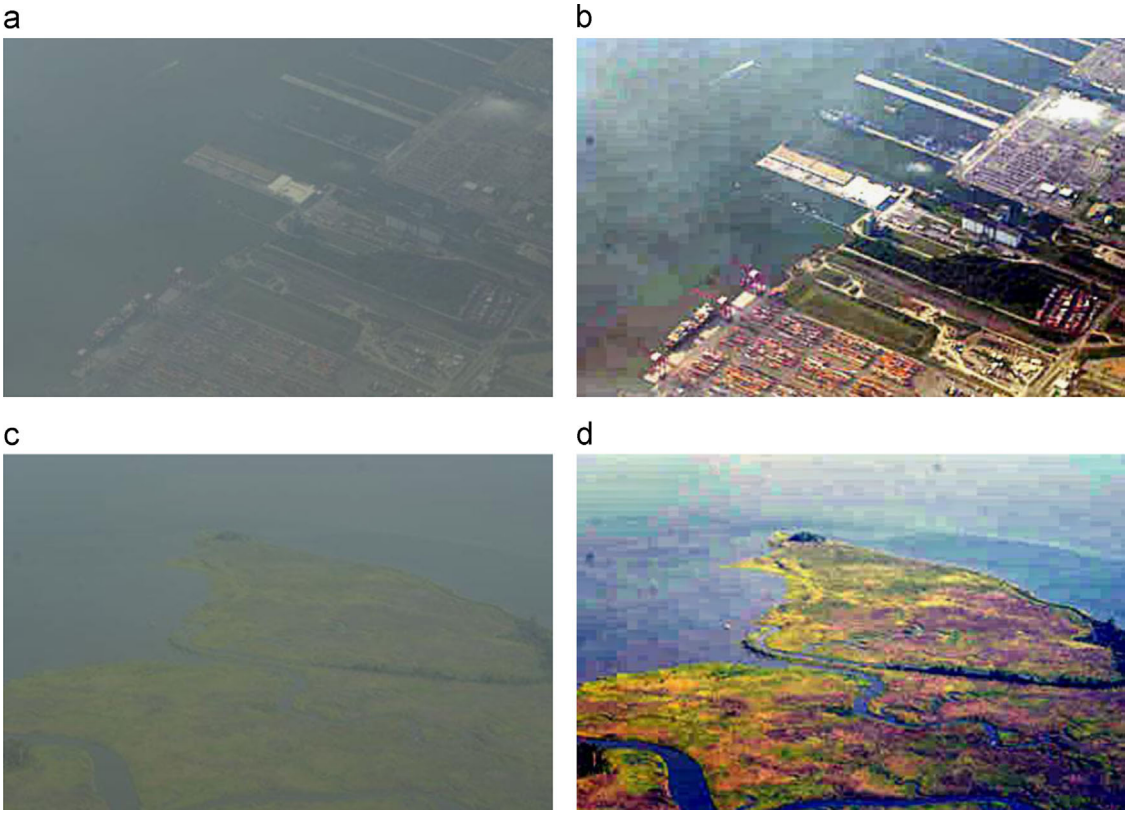

Fig. 2. MSRCR [14]'s success and failure. Success: for the original image (a), the lightness and contrast are greatly improved in its enhanced result (b). Failure: the image (c) is enhanced too much, blocking effects and color distortion appear in the result (d).

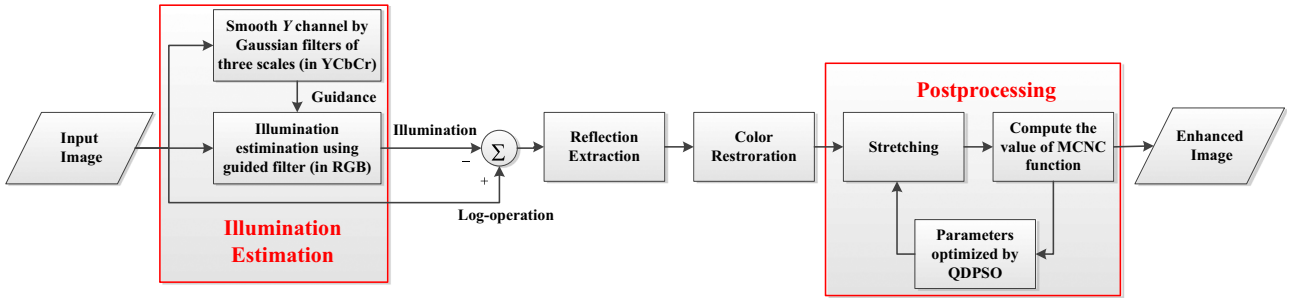

Fig. 3. The pipeline of the proposed algorithm.

most of the details (see Fig. 2(a) and (b)), a large number of parameters are involved and set empirically, such as the scales and weights of Gaussian filters, and stretching factors, which limits the generalization ability and often results in pseudo halos and unnatural color (see Fig. 2(c) and (d)).

Recently, some improvements on MSRCR have been proposed. Rather than utilizing the Gaussian filters to perform the illumination estimation, the method in [17] employs a denoising technique called non-local means filter, assuming that the denoised image is equivalent to the illumination image. In [18], the illumination of the input image is estimated using a guided filter, which not only plays the smoothing role, but also transfers the structure of its guidance image to the filtering output. Jang et al. [19] propose the visual contrast measure (VCM) method to select the scales and weights of Gaussian filters for illumination estimation, while the parameters of MSRCR in [20] are optimized using the particle swarm optimization (PSO) method. Apart from the obtained reflectance, the mid-tone of the image is also considered in [21] by applying an inverse sigmoid function to the estimated illumination.

This paper focuses on improving the visual quality of outdoor images, especially for those captured under the overcast or low-light conditions. To this end, we propose a biologically inspired adaptive image enhancement method. The pipeline of the proposed method is shown in Fig. 3.

Firstly, we also exploit guided filter to estimate the illumination. However, different from [18] which directly uses the input image as the guidance image of the guided filter, we utilize the smoothed Y channel in the YCbCr color space, which can better reflect the luminance of the real scene. The smoothing operation of the Y channel is conducted by utilizing a weighted combination of three Gaussian filters with different scales, the weights of which depend on the local contrast [19] of the Y channel. According to the estimated illumination, the reflection of the input image is then predicted using the Retinex algorithm. Finally, the predicted reflection is further refined via color restoration followed by a novel automatic postprocessing method to obtain the final enhanced image. Specifically, in the postprocessing stage, we explore a learning strategy to select the optimal parameters of the nonlinear stretching by optimizing a novel image quality measurement, named as the Modified Contrast–Naturalness–Colorfulness (MCNC) function. Compared with the original CNC function [22], the proposed MCNC function employs a more effective objective criterion and thus better agrees with human visual perception. The optimization of parameters is conducted by using the QDPSO method [23], which has a stronger ability of global searching than the PSO method utilized in [20].

The contributions of this paper can be summarized as follows:

(1) We propose a novel design for the guided filter by utilizing the smoothed Y channel in the YCbCr color space as the guided image, which can reflect the luminance of the real scene and facilitates a better estimation of the illumination.
(2) We propose the MCNC function for the evaluation of image quality, which is more effective and better accord with the human visual perception than the CNC function considering both color and contrast of images.
(3) We explore a novel and effective postprocessing method, where the parameters of the stretching are adaptively determined by maximizing the value of MCNC function.

The remainder of this paper is organized as follows: the multi-scale Retinex with color restoration (MSRCR) method is explained in Section 2. In Section 3, a novel biologically inspired image enhancement method based on Retinex is proposed. Both quantitative and qualitative experimental results are reported in Section 4. Section 5 summarizes our work.

2. Multi-scale Retinex with color restoration (MSRCR)

According to the Retinex theory [11], the visual rendering of an image relies on two factors: the distribution of the source illumination and that of the scene reflectance, where the latter has a strong correlation with the sensations of color for the human visual system. Since human eyes exhibit a logarithmic response to the lightness, image enhancement based on the Retinex theory is performed by

$$R(x,y) = \log\ I(x,y) - \log\ L(x,y), \tag{1}$$

where I is the image; (x,y) denotes pixel coordinate; L is the illumination and R is the Retinex output.

Note that the calculation of the illumination L is a singularity problem. In [13,14], the illumination is approximated by filtering the image with the Gaussian surround function, and the color image enhancement is conducted using the single-scale Retinex (SSR) [13] as

$$R_i = \log\ I_i(x,y) - \log\{F(x,y) * I_i(x,y)\}, \tag{2}$$

where $i \in \{r,g,b\}$ and I_i is the ith channel of the input image; R_i is the ith channel of the SSR's output; "$*$" represents the convolution operation; $F(x,y)$ is the Gaussian surround function which is defined as

$$F(x,y) = \frac{1}{\sqrt{2\pi}c}\exp\left\{-\frac{x^2+y^2}{2c^2}\right\}, \tag{3}$$

where the scale c of the Gaussian filter has an important impact on the result [14,19]. Specifically, a small-scale Gaussian filter can well preserve the information of the objects' shape in the estimated illumination, which leads to prominent details in the output, but may easily cause halos and color distortion. On the contrary, a large-scale Gaussian filter can well preserve the image color, but fails to maintain the local contrast and object shape information.

In order to provide both dynamic range compression and tonal rendition simultaneously, the multi-scale Retinex with color restoration (MSRCR) [14] exploits a weighted combination of three Gaussian filters with different scales to conduct color image enhancement by

$$R_{msrcr_i} = G\left\{ C_i(x,y)\left(\sum_{k=1}^{3} \omega_k R_{i,c_k}\right) + t \right\}, \tag{4}$$

where R_{i,c_k} is the output of the SSR method computed by Eq. (2) using the Gaussian filter whose scale is c_k; ω_k is the corresponding weight; G and t are the gain and the offset for stretching adjustment, respectively; $C_i(x,y)$ is the color restoration function of the ith ($i \in \{r,g,b\}$) channel defined as

$$C_i(x,y) = \beta\left\{ \log[\alpha I_i(x,y)] - \log\left[\sum_{i \in \{r,g,b\}} I_i(x,y)\right]\right\}, \tag{5}$$

where β is a gain constant and α controls the strength of the nonlinearity.

Though the MSRCR algorithm has strong abilities of providing good dynamic range compression and preserving most of the details, there are too many parameters involved [14], such as the scales and weights of Gaussian filters, the gain and offset parameters in the stretching. Besides, all the parameters are empirically set, which decrease the robustness of the MSRCR algorithm and often result in pseudo halos. In order to handle this issue, our method explores a learning strategy to adaptively determine the parameters for each input image and achieves more robust performance.

3. Enhancement algorithm

In this section, we present a biologically inspired adaptive image enhancement method, which consists of the following three steps: (1) illumination estimation using a newly designed guided filter, (2) reflection extraction followed by color restoration, and (3) postprocessing.

3.1. Illumination estimation

The guided filter [24] performs smoothing operator which can transfer the structure of the guidance image to the filtering output. Given an input image in YCbCr color space, we estimate the illumination of the image using guided filter with the Y channel as the guidance image, which can better reflect the luminance of the real scene. In practice, we observe that the Y channel contains rich local boundary details, which could cause redundant information to be transferred if directly used as the guidance image, so a smoothing operation over the Y channel is necessary.

Following [14], the smoothing operation is performed by a weighted combination of three Gaussian filters, whose scales are $c_1 = 240$, $c_2 = 80$ and $c_3 = 15$. The corresponding weights are determined by $w_1 = (2*P+1)/3$, $w_2 = w_3 = (1-w_1)/2$, where P is the normalized local contrast [19] of the Y channel computed as

$$P = 1 - \frac{1}{\overline{m}}\sqrt{\frac{1}{N_b}\sum_{l=1}^{N_b}(m_l - \overline{m})^2}, \tag{6}$$

where N_b is the number of divided sub-blocks; m_l represents the average luminance of the lth sub-block; and $\overline{m}$ indicates the average luminance of the Y channel. The smoothing process can then be performed by the combination of three Gaussian filters as

$$Y_f(x,y) = \sum_{k=1}^{3} \omega_k \{F_k(x,y) * Y(x,y)\},$$

$$F_k(x,y) = \frac{1}{\sqrt{2\pi}c_k}\exp\left\{-\frac{x^2+y^2}{2c_k^2}\right\}, \tag{7}$$

where F_k is the kth Gaussian filter whose scale and weight are c_k and w_k, respectively. Using Y_f as the guidance image, the illumination is estimated by applying the guided filter to the input image as follows:

$$L_i(x,y) = \frac{1}{|w^{(x,y)}|}\sum_{(u,v)\in w^{(x,y)}}\left\{a_i^{(u,v)}Y_f(x,y) + b_i^{(u,v)}\right\}, \tag{8}$$

where L_i is the ith ($i \in \{r,g,b\}$) channel of the estimated illumination; Y_f is the smoothed Y channel of the input image, which is utilized as the guidance image; $w^{(x,y)}$ denotes the local square window centered at (x,y); $|w^{(x,y)}|$ denotes the number of pixels in $w^{(x,y)}$; $a_i^{(u,v)}$ and $b_i^{(u,v)}$ are some linear coefficients computed as

$$a_i^{(u,v)} = \frac{\frac{1}{|w^{(u,v)}|}\sum_{(k,j)\in w^{(u,v)}} I_i(k,j)Y(k,j) - \mu_i^{(u,v)}\mu_Y^{(u,v)}}{(\sigma_Y^{(u,v)})^2 + \varepsilon},$$

$$b_i^{(u,v)} = \mu_i^{(u,v)} - a_i^{(u,v)}\mu_Y^{(u,v)}, \tag{9}$$

where I_i is the ith ($i \in \{r,g,b\}$) channel of the input image; $\mu_i^{(u,v)}$ is the mean of I_i in $w^{(u,v)}$; $\mu_Y^{(u,v)}$ and $(\sigma_Y^{(u,v)})^2$ are the mean and variance of Y_f in $w^{(u,v)}$, respectively; ε is a regularization parameter. In all the reported experiments, the size of each local square window is set to 30×30 pixels, and the regularization parameter ε is set to 0.01.

Fig. 4 shows the robustness of the proposed method in predicting the illumination. The illumination of the input image (Fig. 4(a)) is dim and uniform. The illumination estimated by the method of [14] demonstrates redundant information of the local boundaries, which do not belong to the distribution of the illumination and may lead to excessive enhancement and halos in the final result (Fig. 4(c)). Since our method adopts the smoothed Y channel (Fig. 4(d)) as the guidance image, the estimated illumination (Fig. 4(e)) can better reflect the uniform distribution of the real scene, which makes the final enhanced image (Fig. 4(f)) more clear and natural.

3.2. Reflection extraction and color restoration

After estimating the illumination, the reflection of the image is extracted from the original image as follows:

$$R(x,y) = \sum_{i\in\{r,g,b\}} \log\, I_i(x,y) - \log\, L_i(x,y), \tag{10}$$

where I_i and L_i are the ith ($i \in \{r,g,b\}$) channel of the input image and illumination, respectively; $R(x,y)$ is the logarithmic distribution of scene reflectance.

Considering a color restoration scheme that provides good color rendition for images containing gray-world violations, Eq. (10) is modified [14] as follows:

$$R(x,y) = \sum_{i\in\{r,g,b\}} C_i(x,y)\{\log\, I_i(x,y) - \log\, L_i(x,y)\} \tag{11}$$

where C_i is the color restoration function for the ith channel, which is computed as Eq. (5). In our experiment, we empirically set the parameters of C_i as $\beta = 1$ and $\alpha = 125$.

3.3. Postprocessing

In the MSRCR method [14], the final output is obtained by using a pair of gain and offset constants G and t (in the Eq. (4)) for the transition between the logarithmic domain and the display domain. However, we argue that such a global linear stretching sometimes cannot provide prominent details for the region of interest. In order to address this issue, we propose a novel automatic postprocessing method, which consists of nonlinear stretching and parameters optimization. Specifically, the

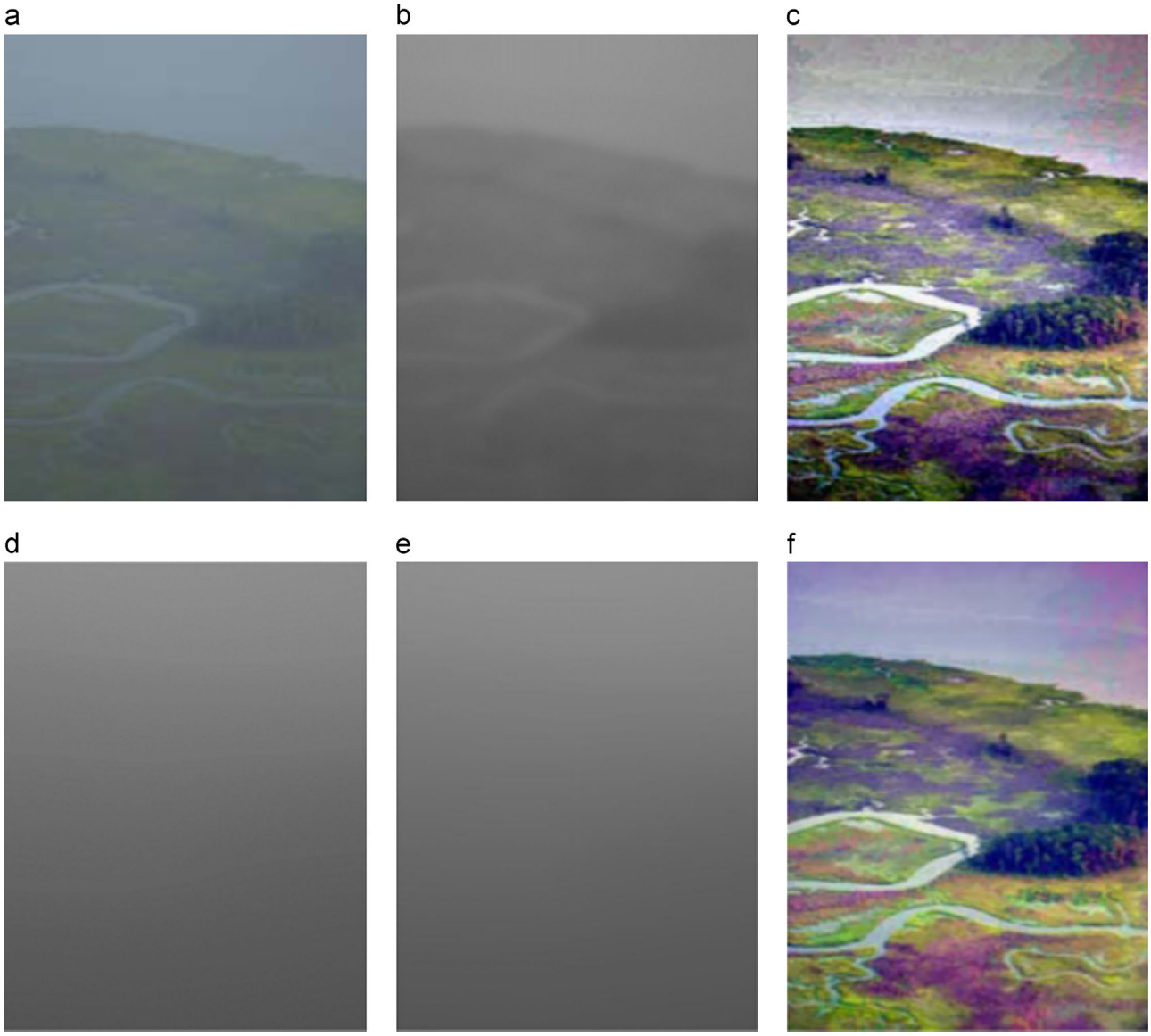

Fig. 4. Illumination estimation. (a) Original image, (b) illumination estimated by [14], (c) enhanced result of [14], (d) guidance image Y_f, (e) illumination estimated by our method, and (f) enhanced result of ours.

parameters of the stretching are learned by maximizing the MCNC value (see Section 3.3.2) of the output image, which is efficiently solved by using the QDPSO algorithm (see Section 3.3.3).

3.3.1. Stretching

Fig. 5 shows the statistic curve of the cumulative distribution function (CDF) [25] of pixel intensity values in natural images. It can be observed that only a few pixel values of images are in a saturated state, and the majority fall in the range of $[R^{low}, R^{high}]$, where R^{low} and R^{high} denote the lower and upper saturated points, respectively. In addition, those pixels in the saturated state have little impact on the whole image.

In order to highlight the main details of the image, we only stretch those pixels whose values fall into the range of $[R^{low}, R^{high}]$ by gamma correction [26] as follows:

$$R_i^{out} = \begin{cases} 0 & R_i(x,y) < R_i^{low} \\ 255\left(\dfrac{R_i(x,y) - R_i^{low}}{R_i^{high} - R_i^{low}}\right)^{\gamma_i} & R_i^{low} \le R_i(x,y) \le R_i^{high} \\ 255 & R_i(x,py) > R_i^{high} \end{cases}, \tag{12}$$

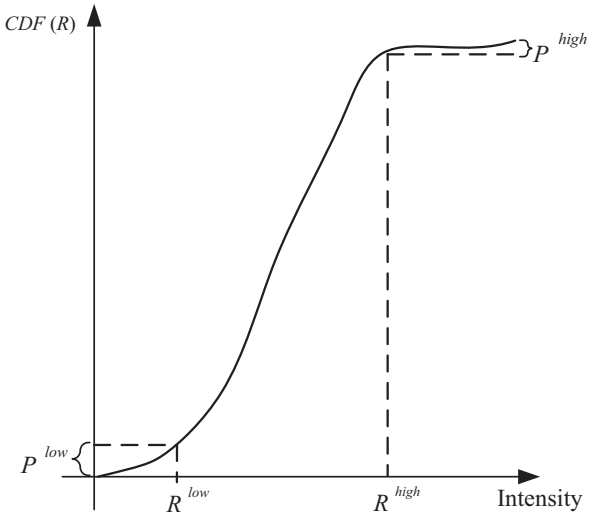

Fig. 5. The cumulative distribution function.

where $i \in \{r, g, b\}$, $R_i(x, y)$ is the ith channel of logarithmic distribution of scene reflectance after color restoration computed by Eq. (11). When the value of the gamma coefficient [27] γ_i is greater than 1, the correction produces a concave downward function, and consequently bright parts of the image are compressed and the dark parts are extended; while the value is less than 1, the opposite effects are produced. The saturated points R_i^{low} and R_i^{high} of the ith channel are estimated as follows:

$$R_i^{low} = \mu_i - val \cdot \sigma_i,$$
$$R_i^{high} = \mu_i + val \cdot \sigma_i, \tag{13}$$

where μ_i and σ_i are the mean and the mean-square deviation of the pixel intensities in the ith channel, respectively; and *val* is a truncation factor. It is observed in our experiments that both the gamma coefficient γ_i and the truncation factor *val* directly have significant influence on the contrast and lightness of the enhanced image. Different from [28] where the truncation factor is fixed for all the input images, we employ an adaptive learning method to determine the optimal values of γ_i and *val* for each image by maximizing the value of the modified Contrast–Naturalness–Colorfulness (MCNC) function (described in Section 3.3.2). Thus, our method is more robust and can obtain pleasant enhanced results for various kinds of degraded outdoor images.

3.3.2. Modified Contrast–Naturalness–Colorfulness (MCNC) function

The human vision system is highly sensitive not only to the contrast, but also to the color quality [22] which measures both the naturalness and colorfulness of the images [29]. As an objective measurement for image quality, the Contrast–Naturalness–Colorfulness (CNC) function [22] achieves favorable performance against other methods [30–32] by simultaneously considering the following three indexes: contrast, naturalness and colorfulness. In practice, however, we found that the measurement of contrast in [22], computing the ratio of the cardinal numbers of visible edges of the enhanced image and the input image, cannot work well when block effects appear or some noise is enhanced in the result images. Thus we modify it by adopting an efficient objective criterion [20,33]. The definitions of the three indexes are listed below:

Contrast: In [20,33], the contrast of the enhanced image is assessed by the performance measures including entropy, sum of edge intensities and number of edge pixels. We measure the modified contrast index (MCI) in a similar way as follows:

$$\mathrm{MCI}(I) = \log(\log(E(I_{vis})) \times \frac{n_e(I_{vis})}{M \times N} \times H(I_{vis}), \tag{14}$$

where I is the gray-level of the enhanced image of $M \times N$ pixels; I_{vis} is the visible edge image of I, which is computed as [30]; $E(\cdot)$ represents the sum of intensities; $n_e(\cdot)$ denotes the number of

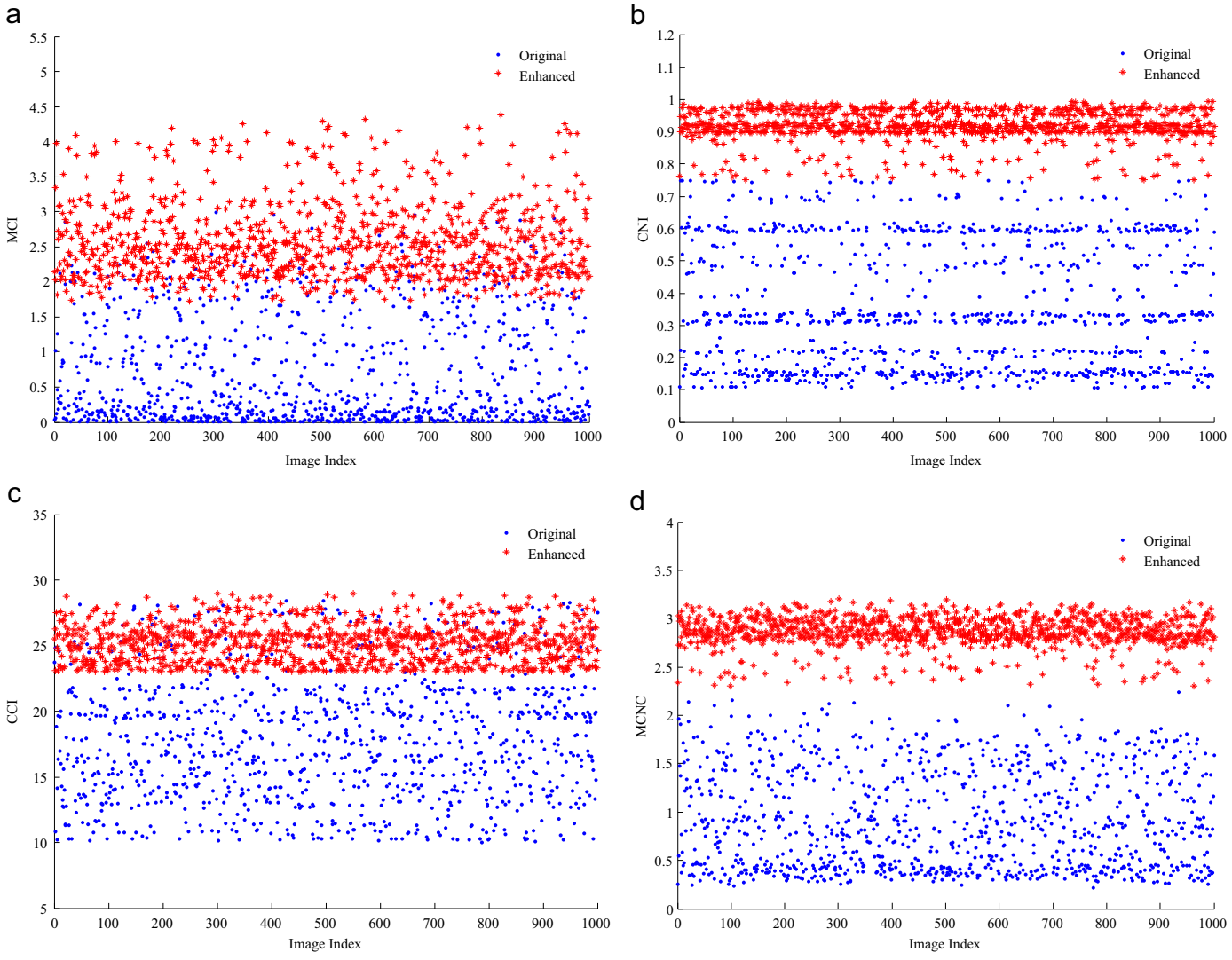

Fig. 6. The statistical results of (a) MCI, (b) CNI, (c) CCI and (d) MCNC of 1000 original image and their enhanced results. (For interpretation of the references to color in this figure, the reader is referred to the web version of this paper.)

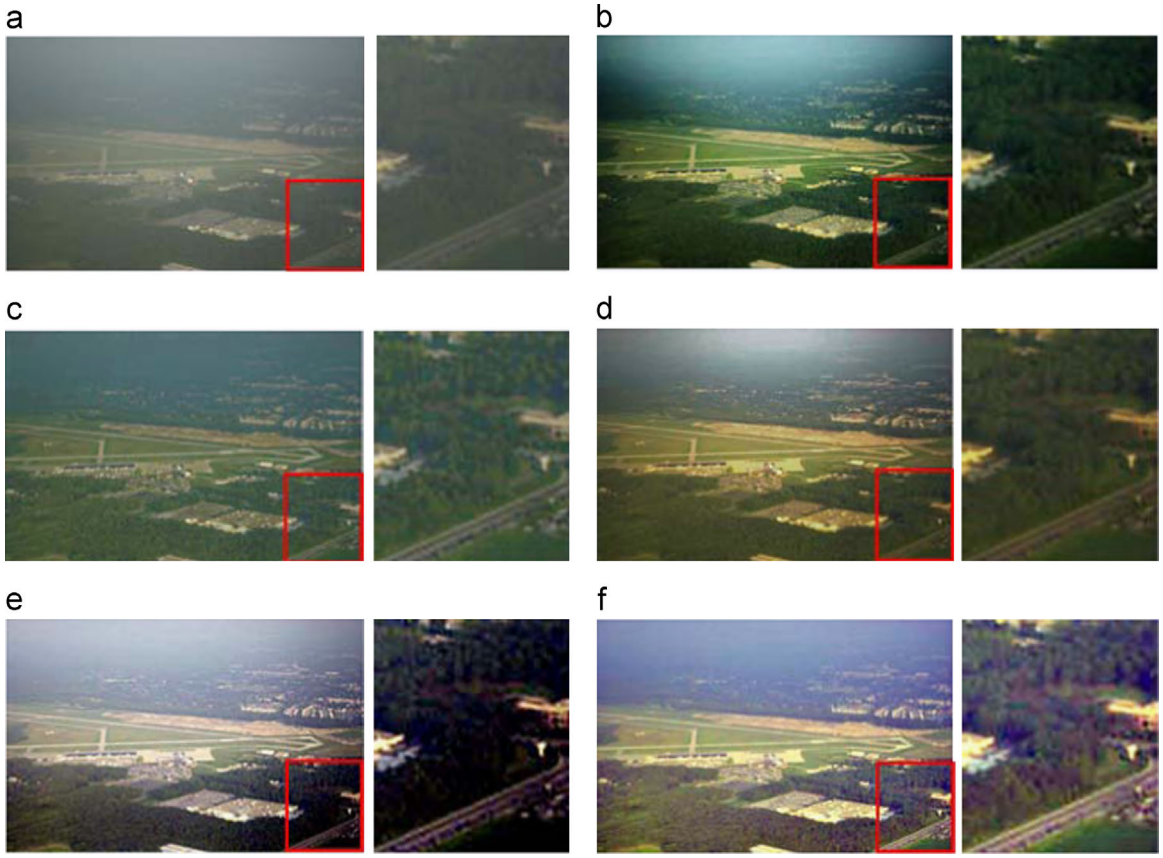

Fig. 7. Haze Example 1. (a) Original image and its results processed by the (b) DCP [4], (c) Visibresto [5], (d) WD [7], (e) MSRCR [14] and (f) proposed. The regions (indicated by red bounding box) are zoomed in and demonstrated on the right. (For interpretation of the references to color in this figure caption, the reader is referred to the web version of this paper.)

edges; and $H(\cdot)$ indicates the entropy value of the histogram. Note that, though in a similar spirit, the proposed contrast measurement differs from [20,33] in that we utilize the visible edge map [30] rather than the Sobel or Canny edge detector, since the former is more consistent with the human vision.

Naturalness: The naturalness of the image indicates the degree of correspondence between human perception and the reality world [29,34]. In this paper, the color naturalness index (CNI) is evaluated using the method in [29], and belongs to range of $[0, 1]$. As CNI increases towards 1, the color of the image becomes more natural.

Colorfulness: The colorfulness of the image, denoted as CCI, reflects the richness and vivid degree of color [29,34] and is measured by the metric proposed in [35]. When CCI is in the range of $[20, 30]$, the color of image is suitable for human vision [34].

The modified CNC function incorporating the three indexes above is defined as

$$\mathrm{MCNC}(I) = (\mathrm{MCI}(I)^{1/n_1} + \mathrm{CCI}(I)^{1/n_2}) \times \mathrm{CNI}(I), \tag{15}$$

where the hyperparameters n_1 and n_2 are both set to be 5 according to [22].

An image with good quality, i.e., with high contrast, natural and vivid color which are consistent with the human vision, should have a high MCNC value. Therefore, we employ the MCNC function of the output image as the objective function, which is maximized to obtain the final enhanced image and the corresponding optimal parameters (the gamma coefficient γ_i and the truncation factor *val*). The optimization process is conducted by the QDPSO algorithm, which is an effective optimization method and will be explained next.

3.3.3. Parameter optimization by QDPSO

Based on the above observation, we formulate the searching for the optimal parameters as the maximization of the MCNC function as follows:

$$\begin{aligned} &\langle \gamma_r^*, \gamma_g^*, \gamma_b^*, val^* \rangle = \arg \max_{\gamma_r, \gamma_g, \gamma_b, val} \mathrm{MCNC}(R^{out}(\gamma_r, \gamma_g, \gamma_b, val)), \\ &\text{s.t.} \quad 0.5 \le \gamma_i \le 2.0, \quad i \in \{r, g, b\} \\ &2.5 \le val \le 3.0 \end{aligned} \tag{16}$$

where γ_i represents the gamma coefficient for the ith color channel; *val* denotes the truncation factor (shared across different color channels); and $R^{out}(\gamma_r, \gamma_g, \gamma_b, val)$ is the enhanced output computed by Eq. (12) with parameters γ_r, γ_g, γ_b and *val*. We solve the optimization problem in Eq. (16) using the quantum delta-potential-well-based particle swarm optimization (QDPSO) method [23]. Specifically, the four parameters are treated as the 4-D position of a particle. The position of the particles are first randomly initialized according to the constraints in Eq. (16). In each iteration, the particle with the maximal MCNC value is regarded as the current best one, that is, its corresponding enhanced image is currently better than the others with respect to the quality of contrast, naturalness and colorfulness. The locations of all particles are updated until the termination criterion is met. Then the current best particle in the last iteration is the global optimal one, whose corresponding enhanced image is most consistent with the human vision and will be output as the finally enhanced image. Detailed algorithm is outlined in Algorithm 1.

Algorithm 1. Biologically inspired image enhancement based on Retinex.

Input: I: the original image; N: the number of particles; K: the number of iterations;

Input: I: the original image; N: the number of particles; K: the number of iterations;

Output: R^{out^*}: the optimal enhanced image;

1: **Illumination Estimation:**

2: Convert I from RGB to YCbCr color space, and obtain the guidance image Y_f according to (6) and (7);

3: Estimate the illumination L in the RGB color space according to (8) and (9);

4: Extract the reflection R, and refine it through color restoration according to (11);

5: **Postprocessing:**

6: Initialization: random $X_n(0)=[\gamma_{r,n},\gamma_{g,n},\gamma_{b,n},val_n](n=1,2,\ldots,N)$; $k=0$;

7: **while** $(k\le K)$ **do**

8: Stretch R with parameters $X_n(k)$ according to (12), and get the enhanced images $R_n^{out}(k)(n=1,\ldots,N)$;

9: Compute the MCNC($R_n^{out}(k)$) for each $R_n^{out}(k)$ according to (15);

10: Select the current global best stretched image as $R_{best}^{out}(k)$:

Input: I: the original image; N: the number of particles; K: the number of iterations;

$pbest_n(k)=\arg\max \mathrm{MCNC}(R_n^{out}(j)), j=1,2,\ldots,k$

$R_{best}^{out}(k)=\arg\max \mathrm{MCNC}(pbest_n(k)), n=1,2,\ldots,N$

11: Update all the $X_n^{(k)}(n=1,2,\ldots,N)$ according to [23];

12: $k=k+1$;

13: **end while**

14 $R^{out^*}=R_{best}^{out}(K)$;

15: **return** R^{out^*};

4. Experiments and results

In this section, experiments and evaluations are conducted from three aspects. We first evaluate the robustness of the proposed method on a large dataset, and then compare our method with state-of-art algorithms qualitatively and quantitatively on some specific instances.

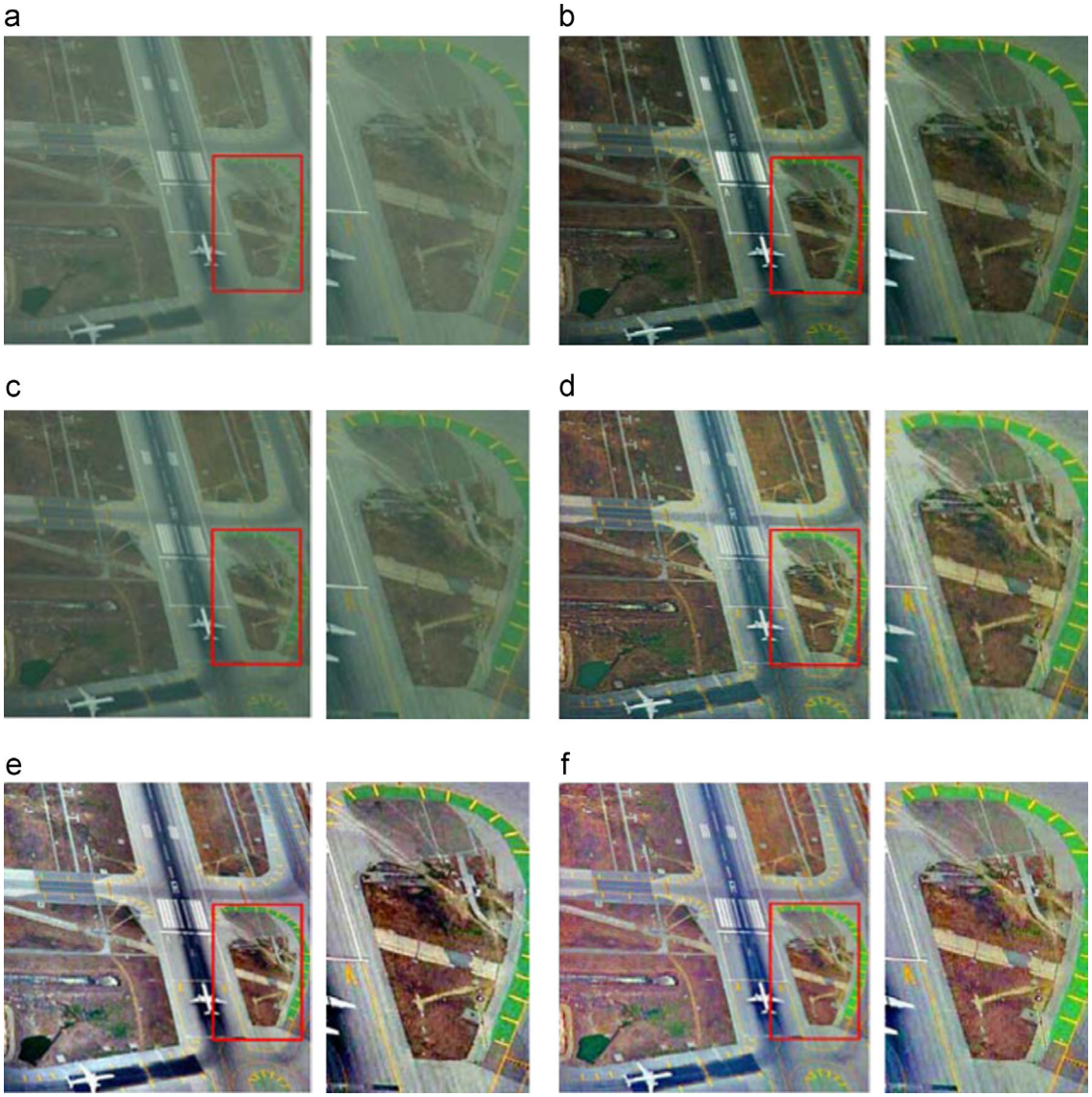

Fig. 8. Haze Example 2. (a) Original image and its results processed by the (b) DCP [4], (c) Visibresto [5], (d) WD [7], (e) MSRCR [14] and (f) proposed. The regions (indicated by red bounding box) are zoomed in and demonstrated on the right. (For interpretation of the references to color in this figure caption, the reader is referred to the web version of this paper.)

4.1. Evaluation on a large dataset

To validate the robustness of our image enhancement method, especially the proposed guided filter (Section 3.1) and the parameter optimization technique (Section 3.3.3), we evaluate the proposed method on a large dataset consisting of 1000 images randomly sampled from 27 aerial videos. Each image demonstrates a different outdoor scene, which makes our dataset cover 1000 different outdoor scenes in total.

We use four indexes to quantitatively evaluate the performance of our method, including the contrast MCI, the naturalness CNI, the colorfulness CCI and the MCNC values (see Section 3.3.2). As mentioned above, with the increase of the value of CNI towards 1, the image looks more natural. When the value of CCI is within [20, 30], the colorfulness of the image is moderate to human eyes. When the contrast and color quality of the image are improved, the values of both MCI and MCNC will increase. Fig. 6 depicts the statistical results, where the blue dots stand for original images and the red asterisks for the enhanced results. It is clear that the four indexes of the original images are distributed randomly with low values, while the indexes of the enhanced results are clustered with high values. The results show that our method is effective and robust to various kinds of outdoor scenes, which can be attributed to the adaptive parameter optimization approach and that the guidance image we utilized for the guided filter can better reflect the luminance of the real scene.

4.2. Qualitative evaluation

In this section, two kinds of challenging weather conditions, including overcast and low-light, are considered for qualitative evaluation.

Fig. 9. Low-light examples. (a) Original image, and its results processed by the (b) CLAHE [9], (c) RRE [36], (d) MSRCR [14] and (e) proposed. The regions (indicated by red bounding box) are zoomed in and demonstrated on the right. (For interpretation of the references to color in this figure caption, the reader is referred to the web version of this paper.)

Table 1
CNC, MCNC and e_{vcm} of the result images produced by five methods on two haze examples.

Test image	DCP			Visibresto			WD			MSRCR			Proposed		
	CNC	MCNC	e_{vcm}	CNC	MCNC	e_{vcm}	CNC	MCNC	e_{vcm}	CNC	MCNC	e_{vcm}	CNC	MCNC	e_{vcm}
Suburb	2.25	2.41	2.35	1.64	1.78	1.24	2.14	2.24	2.17	2.22	2.31	3.11	2.56	2.77	3.65
Airport	1.59	1.78	1.31	1.27	1.34	1.15	2.07	2.32	2.39	2.45	2.75	4.88	2.67	2.99	4.23

Table 2
CNC, MCNC and e_{vcm} of the result images produced by four methods on three low-light examples.

Test image	CLAHE			RRE			MSRCR			Proposed		
	CNC	MCNC	e_{vcm}	CNC	MCNC	e_{vcm}	CNC	MCNC	e_{vcm}	CNC	MCNC	e_{vcm}
Bridge	2.08	2.28	7.44	1.59	1.69	4.79	1.72	1.59	8.11	2.09	2.33	8.83
Greenbelt	1.89	1.87	5.19	2.26	2.16	3.99	2.89	2.97	9.24	2.82	3.09	10.05
Lamplight	2.12	2.18	3.93	2.24	2.38	4.34	2.45	2.41	10.53	2.81	3.10	11.59

For the overcast condition, we compare our method with four state-of-art algorithms: the Dark Channel Prior (DCP) method [4], the fast visibility restoration (Visibresto) method [5], the Wiener defog (WD) method [7], and the MSRCR method [14]. Among them, the first three methods are based on the physical model, which can well handle mist but perform poorly for other kinds of degenerations, such as low-light condition. Thus, for the low-light condition, we adopt three other enhancement algorithms for comparison, including the contrast-limited adaptive histogram equalization (CLAHE) [9], Retinex with a robust envelope (RRE) method [36], and MSRCR [14].

Figs. 7 and 8 show two examples under overcast condition, where the original images are both from NASA's web site. From this figure, we can observe that the DCP method performs well on haze removal, but its haze-free results are dark overall with small dynamic range. For the Visibresto method, there still exist residual haze more or less in the results, whose lightness are also insufficient. The WD method performs well on the second example but failed on the first one. Compared to the first three methods which are all based on the physical model, the MSRCR and the proposed method perform better in terms of contrast and lightness. In addition, our results expose more amount of information, and look more pleasant with vivid color and good dynamic range.

Fig. 9 shows three low-light examples, where the first original image is from the internet and the other two are captured by ourselves. Overall, all the four methods work well and improve the visibility of the images. However, the darkness in the results of the MSRCR method and our method is removed more thoroughly. In comparison, the results obtained by our method reveal the most amount of information, with pleasant color quality and contrast.

4.3. Quantitative evaluation

The methods are quantitatively assessed using three indexes which are all based on the human vision system: (1) the Contrast–Naturalness–Colorfulness (CNC) value [22], (2) the Modified Contrast–Naturalness–Colorfulness (MCNC) value (see Section 3.3.2), (3) the e_{vcm} value, which is the ratio of the VCM values [19] of images after and before the enhancement, and (4) the visually optimal area [37]. Among them, CNC is a kind of comprehensive measure system, combining contrast, naturalness and colorfulness of images. Visual contrast measurement (VCM) provides a gross measure of the regional contrast variations. In order to measure the degree of improvement on the contrast, we compute the VCM value for both the original image and its enhanced result, and then take their ratio e_{vcm} as a compare index. The visually optimal area is a region in a 2D space of the mean and the local standard deviation of images. And the quality of lightness and contrast of images belonging to this area are visually optimal.

Table 1 shows the evaluated results of CNC, MCNC and e_{vcm} on the two haze examples in Figs. 7 and 8. we can see that the proposed method achieves the best results regardless of the condition of color, lightness and contrast. Note that in the second row, the e_{vcm} of MSRCR is higher than ours, since the color of the road is little saturated (see Fig. 8(e)).

Table 2 shows the evaluations of CNC, MCNC and e_{vcm} for the three low-light examples in Fig. 9, which also demonstrates the effectiveness of the proposed method compared with the other three enhancement algorithms.

Fig. 10 shows the evaluation in terms of the visually optimal area, where (a) is the result of five methods on the two haze examples and (b) is the result of four methods on the three low-light examples. It can be seen that our enhanced results lie either inside or closest to the visually optimal region and outperform the others, which again indicates that the proposed method is more consistent with human visual systems compared with the others.

Through further analysis, we find that images captured under overcast with extreme haze often suffer from low illumination and poor contrast. Methods based on the physical model often fail under such condition due to the removal of the atmospheric light [4] which plays a important role of lighting the scene. Especially when there exist some white objects in the original image, the atmospheric light is easily overestimated, leading to more dim areas of the result images. As for the MSRCR method and the proposed method, they both perform well on improving contrast and lightness, but ours is empirically shown to be superior. For images captured under low-light condition, the proposed method can extract as much information as possible with pleasant color compensation.

5. Conclusion

This paper presents a biologically inspired adaptive image enhancement method, consisting of illumination estimation, reflection extraction, color restoration, and postprocessing. Different from previous works, we utilize the smoothed Y channel as the guidance image for the guided filter, which can better reflect the luminance of the real scene. In order to further improve the robustness of our method, we devise a learning scheme to

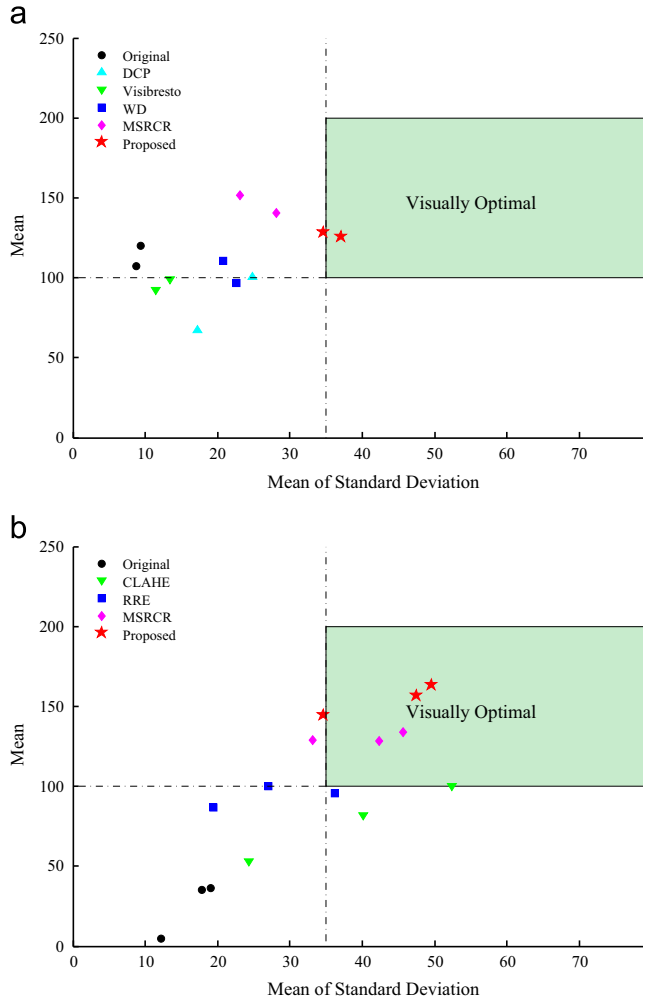

Fig. 10. Visually optimal evaluation. The comparison of methods on the (a) haze examples, and (b) low-light examples.

adaptively determine the optimal value of the parameters for postprocessing by maximization the MCNC function. Numerous experiments show its effectiveness on degraded outdoor images, especially those captured under extremely hazed or low-light conditions. Compared with some state-of-the-art methods both qualitatively and quantitatively, the proposed method is demonstrated to be adaptive and more robust to outdoor images and achieves better performance. In the future, we aim to find a more direct relationship between the parameters of the postprocessing and the MCNC function, rather than utilizing the QDPSO method to conduct the optimization.

Acknowledgment

This research was supported by the Key Laboratory for Aviation Optical Imaging and Measurement, Chinese Academy of Sciences (No. 2012MS04). The authors would like to thank one experienced anonymous referee for his helpful and valuable comments.

References

[1] B. Xie, F. Guo, Z. Cai, Improved single image dehazing using dark channel prior and multi-scale retinex, in: Proceedings of International Conference on Intelligent System Design and Engineering Application, vol. 1, 2010, pp. 848–851.
[2] R.T. Tan, Visibility in bad weather from a single image, in: Proceedings of IEEE Conference on Computer Vision and Pattern Recognition, 2008, pp. 1–8.
[3] R. Fattal, Single image dehazing, ACM Trans. Graph. 27 (3) (2008) 72.
[4] K. He, J. Sun , X. Tang, Single image haze removal using dark channel prior, in: Proceedings of IEEE Conference on Computer Vision and Pattern Recognition, 2009, pp. 1956–1963.
[5] J.-P. Tarel, N. Hautiere, Fast visibility restoration from a single color or gray level image, in: Proceedings of the IEEE International Conference on Computer Vision, 2009, pp. 2201–2208.
[6] J.-P. Tarel, N. Hautire, L. Caraffa, A. Cord, H. Halmaoui, D. Gruyer, Vision enhancement in homogeneous and heterogeneous fog, IEEE Intell. Transp. Syst. Mag. (2012) 6–20.
[7] K.B. Gibson, T.Q. Nguyen, Fast single image fog removal using the adaptive Wiener filter, in: Proceedings of IEEE International Conference on Image Processing, 2013, pp. 714–718.
[8] A.K. Vishwakarma, A. Mishra, Color image enhancement techniques: a critical review, Indian J. Comput. Sci. Eng. 3 (2012) 39–45.
[9] K. Zuiderveld, Contrast limited adaptive histogram equalization, in: Graphics gems IV, Academic Press Professional, Inc., San Diego, 1994, pp. 474–485.
[10] J.-L. Starck, F. Murtagh, E.J. Candes, D.L. Donoho, Gray and color image contrast enhancement by the curvelet transform, IEEE Trans. Image Process. 12 (6) (2003) 706–717.
[11] E.H. Land, J. McCann, Lightness and retinex theory, J. Opt. Soc. Am. 61 (1) (1971) 1–11.
[12] A. Hurlbert, Formal connections between lightness algorithms, J. Opt. Soc. Am. A 3 (10) (1986) 1684–1693.
[13] D.J. Jobson, Z. ur Rahman, G.A. Woodell, Properties and performance of a center/surround retinex, IEEE Trans. Image Process. (1997) 451–462.
[14] D.J. Jobson, Z.-U. Rahman, G.A. Woodell, A multiscale retinex for bridging the gap between color images and the human observation of scenes, IEEE Trans. Image Process. 6 (7) (1997) 965–976.
[15] R. Kimmel, M. Elad, D. Shaked, R. Keshet, I. Sobel, A variational framework for retinex, Int. J. Comput. Vis. (2003) 7–23.
[16] B.V. Funt, F. Ciurea, J.J. McCann, Retinex in matlab, J. Electron. Imaging (2004) 48–57.
[17] A. Choudhury, G. Medioni, Perceptually motivated automatic color contrast enhancement, in: Proceedings of IEEE International Conference on Computer Vision Workshops, 2009, pp. 1893–1900.
[18] H. Ahn, B. Keum, D. Kim, H.S. Lee, Adaptive local tone mapping based on retinex for high dynamic range images, in: Proceedings of IEEE International Conference on Consumer Electronics, 2013, pp. 153–156.
[19] I.-S. Jang, T.-H. Lee, H.-G. Ha, Y.-H. Ha, Adaptive color enhancement based on multi-scaled retinex using local contrast of the input image, in: Proceedings of International Symposium on Optomechatronic Technologies, IEEE, Toronto, 2010, pp. 1–6.
[20] M. Hanumantharaju, V. Aradhya, M. Ravishankar, A. Mamatha, A particle swarm optimization method for tuning the parameters of multiscale retinex based color image enhancement, in: Proceedings of ACM International Conference on Advances in Computing, Communications and Informatics, 2012, pp. 721–727.
[21] L. Tao, R. Tompkins, V.K. Asari, An illuminance-reflectance model for nonlinear enhancement of color images, in: Proceedings of IEEE Computer Society Conference on Computer Vision and Pattern Recognition-Workshops, 2005, p. 159.
[22] F. Guo, J. Tang, Z.-x. Cai, Objective measurement for image defogging algorithms, J. Cent. South Univ. 21 (2014) 272–286.
[23] J. Sun, W. Xu, B. Feng, Adaptive parameter control for quantum-behaved particle swarm optimization on individual level, in: Proceedings of IEEE International Conference on Systems, Man and Cybernetics, vol. 4, 2005, pp. 3049–3054.
[24] K. He, J. Sun, X. Tang, Guided image filtering, IEEE Trans. Pattern Anal. Mach. Intell. 35 (6) (2013) 1397–1409.
[25] K.-q. Huang, Z.-y. Wu, Q. Wang, The application of color constancy to color image enhancement, J. Appl. Sci. 3 (2004) 012.
[26] N. Kwok, H. Shi, Q. Ha, G. Fang, S. Chen, X. Jia, Simultaneous image color correction and enhancement using particle swarm optimization, Eng. Appl. Artif. Intell. 26 (10) (2013) 2356–2371.
[27] A. McAndrew, Introduction to digital image processing with matlab, Chongqing University Press, Chongqing, 2007, pp. 55–57.
[28] Y.b. Rui, P. Li, J.t. Sun, Method of removing fog effect from images, J. Comput. Appl. 26 (2006) 1.
[29] S.N. Yendrikhovski, F.J. Blommaert, H. de Ridder, Perceptually optimal color reproduction, in: Photonics West'98 Electronic Imaging, International Society for Optics and Photonics, San Jose, 1998, pp. 274–281.
[30] N. Hautière, J.-P. Tarel, D. Aubert, É Dumont, et al., Blind contrast enhancement assessment by gradient ratioing at visible edges, Image Anal. Stereol. J. 27 (2) (2008) 87–95.
[31] Z. Wang, A.C. Bovik, H.R. Sheikh, E.P. Simoncelli, Image quality assessment: from error visibility to structural similarity, IEEE Trans. Image Process. 13 (4) (2004) 600–612.
[32] M. Carnec, P. Le Callet, D. Barba, Objective quality assessment of color images based on a generic perceptual reduced reference, Signal Process.: Image Commun. 23 (4) (2008) 239–256.

[33] A. Gorai, A. Ghosh, Gray-level image enhancement by particle swarm optimization, in: World Congress on Nature & Biologically Inspired Computing, IEEE, Coimbatore, 2009, pp. 72–77.
[34] K.-Q. Huang, Q. Wang, Z.-Y. Wu, Natural color image enhancement and evaluation algorithm based on human visual system, Comput. Vis. Image Underst. 103 (1) (2006) 52–63.
[35] D. Hasler, S.E. Suesstrunk, Measuring colorfulness in natural images, in: Electronic Imaging, International Society for Optics and Photonics, Santa Clara, 2003, pp. 87–95.
[36] C.-T. Shen, W.-L. Hwang, Color image enhancement using retinex with robust envelope, in: Proceedings of IEEE International Conference on Image Processing, 2009, pp. 3141–3144.
[37] D.J. Jobson, Z.-u. Rahman, G.A. Woodell, Statistics of visual representation, in: AeroSense 2002, International Society for Optics and Photonics, Orlando, 2002, pp. 25–35.

Yifan Wang received her B.E. degree, in 2013, from Dalian University of Technology (DUT), Dalian, China. She is currently a M.S. degree candidate majored in Signal and Information Processing in DUT. Her research interest is mainly about image enhancement and dehazing.

Hongyu Wang received the B.S. degree in Electronic Engineering from Jilin University of Technology, China, in 1990, the M.S. degree in Electronic Engineering from Graduate School of Chinese Academy of Sciences, Changchun, China, in 1993, and the Ph.D. degree in Precision Instrument and Optoelectronics Engineering from Tianjin University, Tianjin, China, in 1997. He was an Assistant Professor and an Associate Professor in the Department of Electronic Engineering, Zhejiang University, Zhejiang, China from 1997 to 2004. He is currently a Professor in the institute of Information Science and Communication Engineering, Dalian University of Technology, Dalian, China. His research interests include mobile multimedia communications, algorithmic optimization and performance issues in wireless ad hoc, mesh and sensor networks, cross-layer design and optimization.

Chuanli Yin received the B.S. degree from Jilin architectural and civil engineering institute, Changchun, China, in 2003, and the M.S. degree from Chinese Academy of Sciences, Changchun, China, in 2008. He is now an Associate Professor of digital image processing and doing research on embedded system in Changchun Institute of Optics, Fine Mechanics and Physics, Chinese Academy of Sciences, Changchun, China.

Ming Dai received the B.S. from Changchun University of Science and Technology, Changchun, China, in 1990, and the M.S. degree from Chinese Academy of Sciences, Changchun, China, in 1993. He is a Professor in Changchun Institute of Optics, Fine Mechanics and Physics, Chinese Academy of Sciences, Changchun, China. He is mainly devoted to airborne image processing, and stabilizing foundation bed.